



Identification of Prospective Surface Water Available Zones with Multi Criteria Decision Approach in Kushkarani River Basin of Eastern India

Shahana Khatun^{1*} and Swades Pal²

¹Research Scholar, Department of Geography, University of Gour Banga, Malda, India.

²Department of Geography, University of Gour Banga, Malda, India.

Authors' contributions

This work was carried out in collaboration between both authors. Author SP initially designed the study, wrote the methodology and analysis part. Mapping design is also done by him. Author SK prepared the map and collected secondary and primary data as used here. She supported a lot to the referencing part of this work. She also contributed in the discussion part. Both authors read and approved the final manuscript.

Article Information

DOI:10.9734/ACRI/2016/27651

Editor(s):

(1) Magdalena Valsikova, Horticulture and Landscape Engineering, Slovak University of Agriculture, Nitra, Slovakia.

Reviewers:

(1) Bhavana Umrikar, Savitribai Phule Pune University, Pune, Maharashtra, India.

(2) D. O. Ogagarue, Federal University of Petroleum Resources, Effurun, Nigeria.

(3) Kabi Pokhrel, Tribhuvan University, Nepal.

Complete Peer review History: <http://sciencedomain.org/review-history/15430>

Original Research Article

Received 12th June 2016

Accepted 9th July 2016

Published 19th July 2016

ABSTRACT

Present paper mainly intends to find out suitable sites for surface water harvesting in Kushkarani river basin a tributary of Mayurakshi river of Eastern India. For this multiparametric potential surface water availability model and SCS CN based runoff depth models have been prepared in soft ware environments. Both unweighted and weighted linear combination methods are used for compositing the selected parameters. Results show that 14.18% of a total basin area (172 sq. km.) characterised by very high surface water potential is mainly concentrated in the confluence segment of the river followed by high potential zone covering 22.47% area. Unweighted compositing model based estimation shows that very high and high surface water potential zone cover 8.22% and 21.95% of basin area, but areal extent in these two classes is little bit lower than the results obtained from weighted compositing model. Field based discharge measurement validates the surface water potential zones. Similarly, Discharge availability in the rivers of different

*Corresponding author: Email: shahana.khatun1989@gmail.com;

potential zones are also indicating very accordant result and validating the surface water runoff models. SCS CN based runoff depth model represents that 9.32% area covers very high runoff depth (657 mm. to 693 mm). Calculated Relative error value and Nash-Sutcliffe efficiency values are respectively 53.65% and 0.6782 which represent that runoff model is not highly optimum but it is within the range of acceptability. Correlation coefficient value between monsoon runoff depth and surface water potentiality ($r=0.6453$) is high and it is significant at 0.01 level of significance which does indicate both the models are highlighting result in same direction. For validating these models with field based discharge data, it is noticed that discharge data strongly controls surface water availability ($R^2=0.962$) and runoff depth ($R^2=0.970$). From the models it is proved that specifically, confluence segment and very proximate riparian low land of the rivers is selected as suitable sites for surface water harvesting.

Keywords: Surface water potentiality; runoff depth model; discharge measurement; validation of models; suitable sites and surface water harvesting.

1. INTRODUCTION

Water scarcity is likely to be one of the main haunting problems, resulting from combined effects of alterations in the hydrological cycle, anticipated under climate change, and of the increase in water demands for agriculture, urban and industries [1,2]. High population density (756/sq.km. as per Census of India, 2011) and soaring growth of population (1.57%) in the study area is the principal cause behind growing demand of agricultural goods in the study area. To meet the need, in last 40 years, agricultural growth has reached to 4-5% and cropping intensity has raised to 176% [3]. The country like India is highly characterized by seasonal and partially temporal variability of rainfall [4] and this area possesses even more seasonal variability of rainfall. Out of total rainfall, 82% rainfall occurs during June to September [5]. In this high time of rainfall only one crop can be yielded. Rest other cropping intensity is highly supported by irrigation based water supply. Out of total irrigated area 52% irrigated area is served by ground water based irrigation schemes [6] and over time ground water extraction rate for irrigation has been going rise and thereby make the ground water resource scare [7] force ground water table far below ground level (bgl) [8,9]. Events of the failure of ground water extraction by the shallow tube wells established the fact of ground water level is lowering down with very significant scale [10].

In such condition, locating suitable sites for surface water banking and harvesting are essential task for supporting surface water based irrigation projects and sustenance of agricultural production in the study area. The region possesses 234 km. stream length with stream density of 1.41/sq.km. It indicates there is a high

potentiality of surface water availability as runoff. But the entire river basin is not potential for supplying surface water for irrigation. Disparity in stream concentration over space and order of stream usually make a huge difference in surface water availability. For example, stream concentration is high in the upper catchment but most of the streams are either 1st and 2nd orders and therefore water potentiality is very meager.

Present paper attempts to find out the surface water potential sites using multi criteria weighted linear combination (WCL) score in GIS and RS soft wares environment. WLC is done following different approaches as described in method section. In this study tried to validate potential surface water models with discharge data collected from different stream sites and junction sites of various potential water available zones. Apart from this Soil conservation Service Curve Number method is also applied for estimating amount of surface runoff. The SCS CN method is simple and produces better results [11-15]. For simplicity and reliability of this method many researcher used it for runoff estimation. Zhan and Huang [16], Tessema et al. [17], Awadallah et al. [18], Khare et al. [19] have performed this method in GIS environment. In India, Nayak and Jaisawal [20] developed a good correlation between measured and estimated run-off using GIS and SCS CN model. They said that GIS is an effective tool for constructing SCS CN model with maximum input data. In present study SCS CN based surface runoff model is also tried to build up in for the same purpose. Effective runoff depth is calculated from SCS CN based runoff depth model as far the evaporation loss is strongly concerned. Researcher discussed in their study impact of evapotranspiration on runoff and water availability in arid and semiarid plateau region [21].

Applications of remote sensing and GIS for the exploration of groundwater potential zones [22-27] delineation of spatial saturated areas and wetness index [28,29] land use suitability for defining suitable habitat for animal and plant species [30,31], geological favorability [32], suitability of land for agricultural activities [33-35], landscape evaluation and planning [36], environmental impact assessment [37], selecting the best site for the public and private sector facilities [38,39], and regional planning [40] including a number of criteria have been performed and they produced amazing results for concerned decision support. SCS Curve Number [41] based identification of surface water potential zone is also performed by many scholars like Rao et al. and Ramakrishnan et al. [42,43]. This attempt is also useful toward the aim set in this present paper.

2. STUDY AREA

Kushkarani river is an upper catchment tributary of Mayurakshi River situated in Birbhum district of West Bengal and Jamtara district of Jharkhand. The basin is demarcated by 23°54' 36" N. to 24° N. latitudes and 87°14'24" E. to 87°30' E. longitudes with a total area of 172 sq. km. (see Fig. 1). The east-west elongated basin of the 35 km. long river is physiographically situated in the eastern margin of the Chhotanagpur plateau, where the highest elevation (155 metres) is seen in the western side near the source of the river and lowest elevation (62 metres) is seen in the eastern side near its confluence where at present Tilpara barrage and consequent reservoir is located (23°56'46.91"N. lat. and 87°31'30.73"E long.) (see Fig. 1). Maximum area of the basin is occupied by undulated topography with an average elevation of 108 metres. On an average 120 metres contour roughly demarcates upper catchment, 80 metres contour delimits middle and lower catchments. Entire basin area comes under rari tract [44] with secondary laterite formation [45] mainly carried by some of the rivers like Kushkarani coming from Chottanagpur plateau [46-48]. Average slope, measured as per Wentworth's method [49], is 3% to 5% whereas it is <1% in the confluence segment. Geologically 90% of the basin area is composed with granitic gneissic rock of Pleistocene age (50 lakh years old) overlain by coarse grain lateritic soil and a few isolated patches covering 08% and 02% area of the lower catchment is made with older

and newer alluvium respectively of Holocene period over granitic basement (Fig. 1) (GSI 1985). Just below 4 km. below the confluence point Farakka-Midnapore fault passes through. Average annual rainfall of this basin as gauged by Suri meteorological station is 1444.432 mm. High degree of seasonality of rainfall is reflected by 82% rainfall during the months of June to September. Rainfall analysis since 1980 to 2013 focused that there is no significant trend of rainfall as also indicated by linear regression model ($y = -2.137x + 5704$) and coefficient of determination ($R^2 = 0.005$). This trend is identical with the general trend of rainfall in India as estimated by many a scholars. Parthasarathy et al. [50], reported that in all India scale there is no significant change of rainfall in last 110 years excepts few regional pockets. Average potential evaporation of this area since 1901 to 2014 is 73.45 mm./year [51] which indicates one of the controlling factors of surface water.

Most part of the basin is characterized by coarse grain laterite soil with ferruginous nodules, feldspar nodule. In some parts older alluvium admixed with reddish laterite overlain granite gneiss regolith. These soil are very susceptible to erosion and supply substantial amount of sediment to the channel. Extreme confluence segment is characterized by newer alluvium lying over older alluvium and it is because of frequent flooding in response to the water balance to the Tilpara reservoir which is located over Mayurakshi river. Reservoir effects have created back water not only within channel but astride lowlands (see Fig. 1). Backwater effects influence up to 4 km. upstream of Kushkarani river which is the present area of interest.

Total 292 stream segments have identified out of which 224 belongs to 1st order, 55 belong to 2nd order, 12 stream segments belong to 3rd order, and 1 belongs to 4th order. Mean bifurcation ratio of this basin is 4.027. Very less form factor ($F=0.268$) indicates elongated river basin. Drainage frequency, density, texture are respectively 1.695/sq.km., 1.76 km/sq.km and 4.36. Index of areal asymmetry ($A_a=0.754$) indicates asymmetry in area distribution in two sides of the main channel is existing but its degree is very marginal. Hypsometric integral (HI) is 0.38 does indicate the basin is passing through old stage. Positive base level change due to positioning of Tilpara reservoir can shorten cyclic time of this basin.

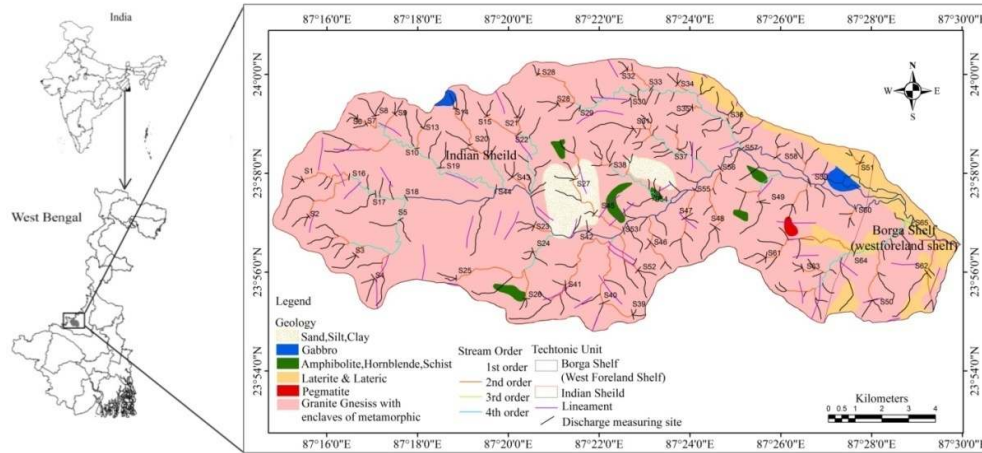


Fig. 1. Study map

3. MATERIALS AND METHODS

For constructing surface water potential zone, thirteen parameters have been considered and their concerned sources are mentioned in Table 1. Data layer used for making SCS CN based runoff model is also mentioned in same table.

3.1 Methods for Surface Water Potential Models

For nearly two decades, a number of multi-attribute (or multi-criteria) evaluation methods have been implemented in the GIS environment for land suitability evaluation, including WLC and its variants [52,53] and the analytic hierarchy process [54]. There are two fundamental classes of multicriteria evaluation methods in GIS: the Boolean overlay operations (noncompensatory combination rules) and the weighted linear combination (WLC) methods (compensatory combination rules). They have been the most often used approaches for different sorts of land-use suitability analysis [55-59]. These approaches can be generalized within the framework of the ordered weighted averaging (OWA) [60-64].

The WLC is a simple additive weighting based on the concept of a weighted average [65]. The decision maker directly assigns weights of 'relative importance' to each attribute map layer. A total score is then obtained for each alternative by multiplying the importance weight assigned for each attribute by the scaled value given to the alternative on that attribute, and summing the products over all attributes. OWA is a family of multicriteria combination procedures [66]. It

involves two sets of weights: the weights of relative criterion importance and the order (or OWA) weights. Although OWA is a relatively new concept [55], there have been several applications of this approach in the GIS environment [61,67-73]. All those applications use the conventional (quantitative) OWA. Specifically, research into GIS, OWA has so far focused on the procedures that require quantitative specification of the parameters associated with the OWA operators.

In the present study thirteen parameters with their spatial pattern have been selected as map layers (see Table 2). Each attribute (map layer) is categorized into 10 classes ranking 1 to 10 (adopting 10 point scale) considering the fact that greater rank will reflect greater potentiality of getting surface water. To fulfill this purpose, all the attributes have been reclassified into 10 classes and ranked accordingly. The logic behind ranking to intra attribute classes from 1-10 is described in Table 2. Weightage of each attribute has been defined objectively (see Table 2) considering the role of those in the study area. The logic behind this consideration is that highly correlated parameter maximally explains the spatial variation of temperature. Normalization of respective weight (values of r for respective parameters) based on dimension index has been done for frame it in a scientific scale. The result of each normalized value is called attribute weight. Weights of the parameters for different season in respective years are different due to having some dynamic variables like land use, canopy coverage etc. Therefore nine prospective models have been articulated for different seasons in the selected years.

Table 1. Spatial parameters and their sources

Parameters	Sources
Drainage frequency, drainage density, slope, sinuosity and pond frequency	Toposheets, Survey of India and Google Image
Weighted junction score	Computed from stream junction map after Pal, 2014
Land use land cover (LULC)	Sensor: Landsat 8 (OLI), Feb., 2014 (Path/Row:139/43; Band used: G, R, NIR; Spatial resolution: 30 m.), Land use map, 2014 of Land reform Deptt., West Bengal
Seasonal and temporal ground water table (GWT)	Central Ground Water Board and State Water Investigating Directorate, 2015
Soil Texture/ soil type	Soil texture map prepared by NIC Birbhum District Centre
Junction buffer and stream line buffer	Prepared from base maps using GIS
Relief parameter	Derived from SRTM data (USGS)
Rainfall	Directorate of Agriculture West Bengal

Expression of weight calculation is as follows:

$$w_j = \frac{a_{jr}}{\sum_{j=1}^n j_r}$$

w_j=weight of jth parameter; a_{jr}= correlation coefficient of jth attribute; $\sum_{j=1}^n j_r$ = summation of correlation of all jth variable.

Rank of all sub classes under each attribute is then multiplied by the defined weight of each individual attribute. This function can be presented using the following formula.

$$WLC = \sum_{j=1}^n a_{ij} w_j$$

Where, a_{ij}= ith rank of jth attribute; w_j= weightage of jth attribute.

This weighted linear combination has been done using raster calculator tool in Arc GIS environment.

Apart from weighted linear combination, same data layers have also used for simple linear combination. This is done for assessing the degree of variation yielded from weighted compositing.

$$LC = \sum_{j=1}^n a_{ij}$$

Where, a_{ij}= ith rank of jth attribute

3.2 Methods for Constructing Employed Data Layers

Each data layer has been constructed in GIS environment using the following methods i.e. drainage frequency and density after Horton [82]. Average slope and classification of relief have been constructed from SRTM data. Land use land cover (LULC) map has been constructed based on Landsat image based supervised image classification in ERDAS Imagine soft ware. The accuracy assessment for supervised technique has made through a confusion or error matrix. Kappa statistics is also calculated for assessing suitability of supervised classification. Total 100 sample sites from Google earth and ground verification are selected for accuracy assessment. The accuracy assessment generated from the supervised classification technique showed an overall classification accuracy was 86.0% with Kappa Statistic of 0.838, which indicates a good agreement between thematic maps generated from image and the reference data. This amount of agreement is generally considered a good statistical return. However, the accuracy of supervised classification is less than 85 %, which is below the acceptable level and standard of digital image classification for optical remote sensing data recommended by Jansen et al. [83]. Agriculture class shows that accuracy level of this class ranges from 77.77% to 91.66%. However, from the result it is found that all land covers classes are classified much better in this supervised approach. Junction buffer and stream line buffer layer have been made using distance mapping techniques in Arc Gis environment.

Table 2. Scaling of parameters, logic behind and their weights based on PCA

Parameters	Scaling	Logic behind scaling	Total correlation score (Xi)	Weighted score (Xi/Ximax)
1. Drainage frequency	10 rank at highest drainage frequency	Surface water potentiality is high at higher frequency class	2.93	0.59
2. Drainage density	10 rank at highest drainage density	High drainage density indicates higher surface water availability.	3.23	0.65
3. Slope	10 rank at low slope	Gentle slope is favorable for stagnating more surface water [74]	4.61	0.93
4. Weighted junction score	10 rank at maximum junction score	Maximum weighted junction is conducive of surface water availability [75]	2.39	0.48
5. LULC	10 rank at healthy water body and vegetation	Healthy vegetation retains maximum water [76]	1.71	0.35
6. GWL fluctuation (temporal)	10 rank at lowest value	Little fluctuation indicates consistency in water level; stable ground water level can support surface water availability [77]	4.32	0.87
7. GWT fluctuation (seasonal)	10 rank at lowest value	Low seasonal fluctuation indicate high level saturation of the upper layer and therefore, chance of water stagnation over surface increases [77]	4.45	0.90
8. Soil texture	10 rank at lowest value	Fine textured soil arrests maximum water [78,79]	1.74	0.35
9. Regional sinuosity	10 rank at highest value	More sinuosity indicates greater length of stream and associated with plain land [80]	2.03	0.41
10. Junction buffer	10 rank at lowest distance	Proximate junction carries high water potentiality	3.24	0.65
11. Stream line buffer	10 rank at lowest distance	Adjacent area of streams possesses high potentiality of water	3.08	0.62
12. Pond frequency	10 rank at highest value	Maximum number of ponds indicate high surface water availability	2.67	0.54
13. Relief	10 rank at lowest value	Low lying area in a basin indicates more surface water potentiality [81]	4.96	1

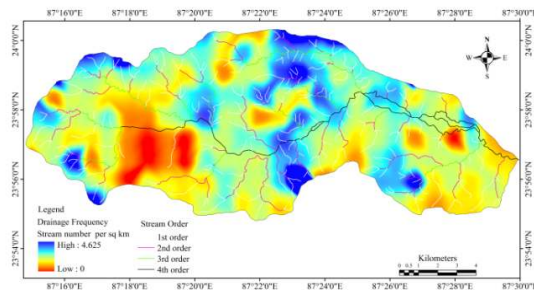


Fig. 2a. Drainage frequency

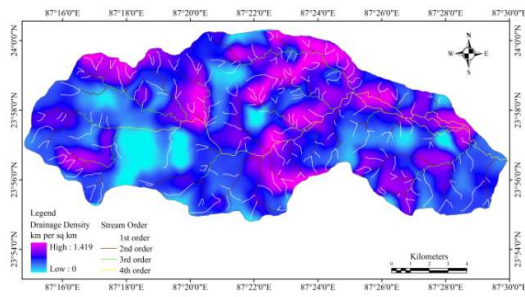


Fig. 2b. Drainage density

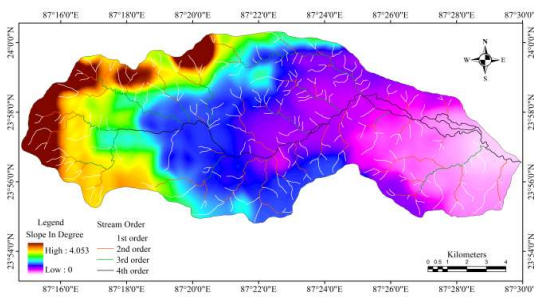


Fig. 2c. Slope map

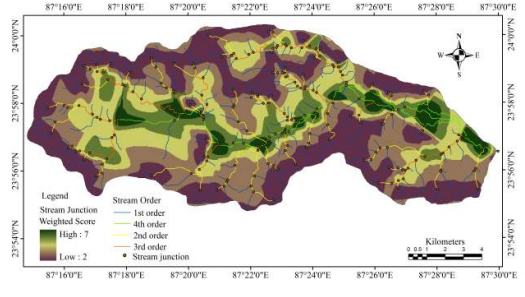


Fig. 2d. Weighted junction score

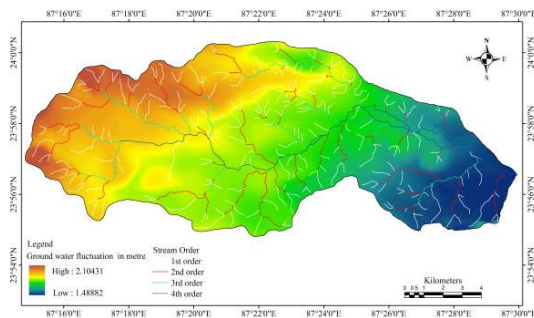


Fig. 2e. Temporal GWT fluctuation (Aug 1990-2014)

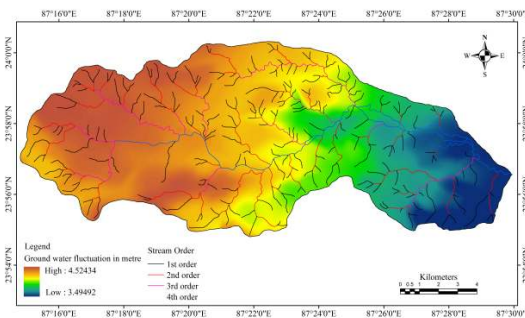


Fig. 2f. Seasonal GWT fluctuation (May-Aug 2014)

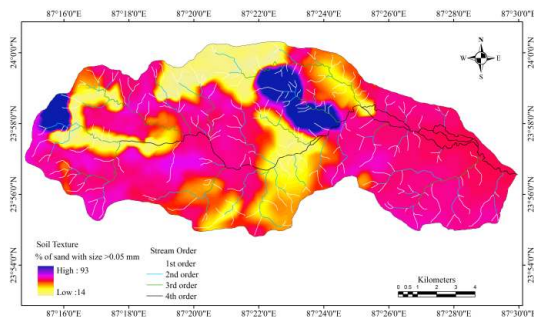


Fig. 2g. Soil texture

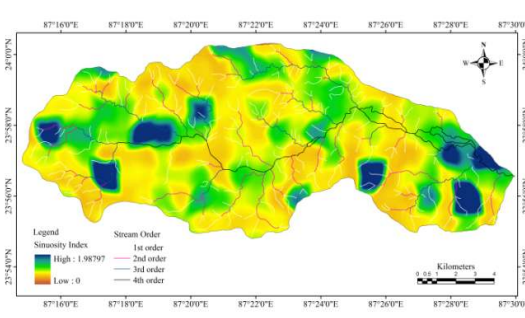


Fig. 2h. Regional sinuosity index

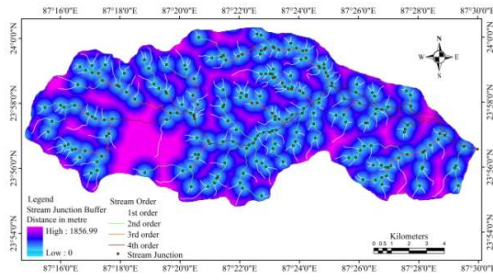


Fig. 2i. Stream junction buffer

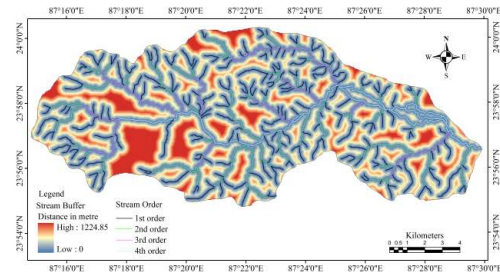


Fig. 2j. Stream line buffer

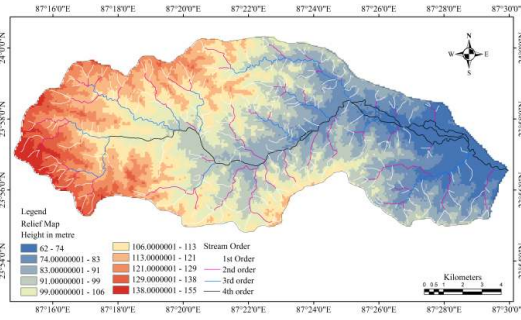


Fig. 2k. Relief map

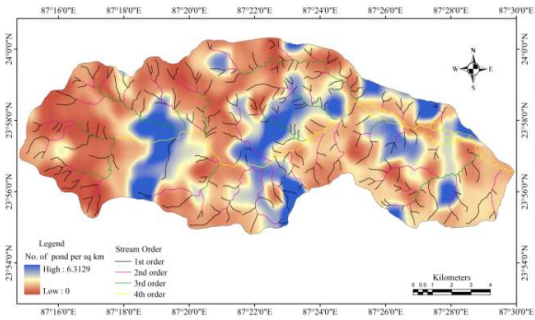


Fig. 2l. Pond frequency

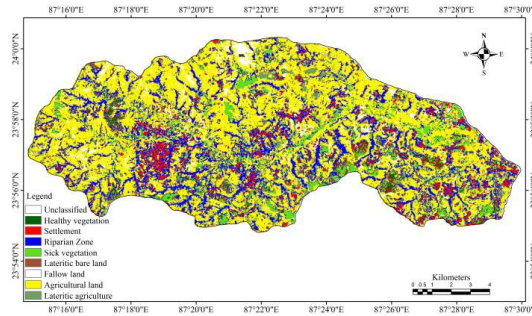


Fig. 2m. LULC

3.3 Method for Estimating Surface Runoff

The SCS model computes direct runoff through an empirical equation that required the rainfall and a watershed co-efficient as input. The watershed co-efficient is called the curve number (CN) which represents the runoff potential of the hydrologic soil cover complexes. The SCS model [84] involves relationships between land cover, hydrologic soil classes and curve number. The equation 1 is used to calculate the surface runoff of a watershed and it is aptly used for small watershed [85].

$$Q = (P - I_a)^2 / (P - I_a + S) \quad (1)$$

Where,

Q is actual surface runoff in mm,
P is rainfall in mm.

For capturing the seasonal variation of initial abstraction I_a should be considered different. Here, for annual runoff modeling, I_a is taken as $0.3S$, for monsoon season it is $0.3S$ and for premonsoon it is $2S$. following Lawrence et al. [86] annual I_a is $0.1S$ [Initial abstraction (mm) or losses of water before runoff begins by soil and vegetation (such as infiltration, or rainfall interception by vegetation)].

S is the potential maximum retention in mm and is calculated using the equation 2.

$$S = (25400 / CN) - 254 \quad (2)$$

Both annual and seasonal runoff depth have been calculated from annual and seasonal rainfall data layers. In earlier section it is mentioned that out of total rain more than 80% rainfall occurs during monsoon period. To capture the impact of seasonal rainfall on runoff, runoff models have been constructed season wise. In runoff model, emphasis is given only on input factors but out factors like evaporation have not considered. Considering this fact effective runoff depth has been calculated deducting evaporation from runoff model.

3.3.1 Discharge data derivation and validation of models

Discharge at different surface water potential zones at different order streams have been measured both during pre and post monsoon. Discharge is measured at 65 sites and stratified sampling technique has been applied to allocate number of sample at different potential zones. Discharge data of different surface water potential zone is corroborated and tried to capture whether discharge data is high at very high or high surface water potential zone. It is considered that if the hypothesis is valid certainly the model will also be validated.

3.3.2 Model validation and runoff predication

The measured runoff is compared with calculated runoff by the SCS-CN model. Subsequently, the applicability of the model is evaluated by testing the relative error (RE) and Nash-Sutcliffe efficiency (NSE) [87], both of which are widely used in evaluation of model performance [88].

$$RE = \frac{(Q_i^{cal} - Q_i^{obs})}{Q_i^{obs}} \times 100\%$$

$$NSE = 1 - \frac{\sum_{i=1}^n (Q_i^{obs} - Q_i^{cal})^2}{\sum_{i=1}^n (Q_i^{cal} - Q_{mean}^{obs})^2}$$

where Q_i^{obs} is the i th observation of runoff, Q_i^{cal} is the i th calculated runoff by the SCS-CN model, Q_{mean}^{obs} is the mean value of observed runoff,

and n is the total number of observations. RE value nearer to 0 indicates high optimality of the model performances. More observed value over calculated value yields negative value. NSE ranges between $-\infty$ and 1, with $NSE = 1$ being the optimal value. Values of NSE between 0 and 1 are generally viewed as acceptable levels of performance, whereas a value of $NSE < 0$ indicates that the mean observed value is a better predictor than the simulated value, which indicates unacceptable performance [88].

4. RESULTS AND ANALYSIS

Both simple and weighted composite surface water availability have been constructed and presented in Figs. 3-4. Figs. 3a and 3b respectively show the simple linear combination based continuous and classified water potential models. Figs. 4a and 4b present the continuous and classified WCL based surface water potential models respectively. Figs. 5a and 6b respectively represent the raster calculators where simple and weighted compositing of the selected parameters have done for generation of models. Tables 3 and 4 depicts the absolute and proportion of area under different potential water availability classes. From the WCL model it is found that out of total area 24.44sq.km or 14.18526% area is characterized by very high potential surface water availability followed by high potentiality 22.48% to total area. 42.40% area is characterized by potential low to very low water availability zones. Potential surface water dearth zone is located at the upper catchment area or gully head zones where slope is relatively stepper ($>3.5^\circ$), drainage density is low (0.4 km./sq.km.), temporal water level fluctuation is relatively high (>1.75 m.). Confluence part of the basin where potential surface water available zone is found is characterized by low altitude (<74 m.), mild slope ($<0.4^\circ$), regional sinuosity is >1.6 , drainage density ranges from 0.4-0.8 km./sq.km., temporal water level fluctuation is <1.5 m. in last 25 years and relatively finer soil texture ($<45\%$ sand with diameter greater than 0.05 mm.). A small depression is also found in this zone where at present Tilpara barrage stores water. Lower part of the basin, very adjacent part of the stream and stream junctions are highly viable areas for harvesting surface water. Agricultural viability is more in this area than upper catchment due to relatively better surface hydrological conditions prevail there on. Surface water support and high soil moisture ($>16\%$) in the pre monsoon months are also some favourable vectors in this regard.

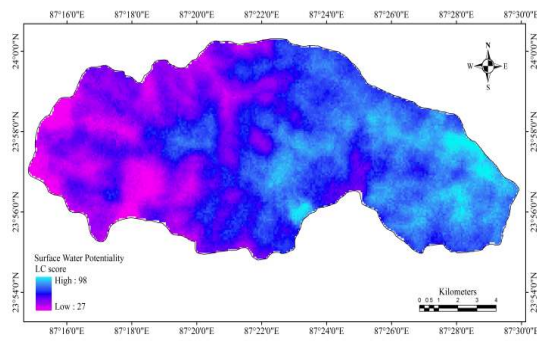


Fig. 3a. Composite surface water potentiality

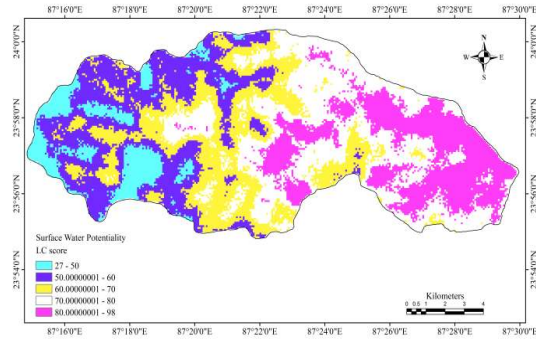


Fig. 3b. Classified surface water potentiality

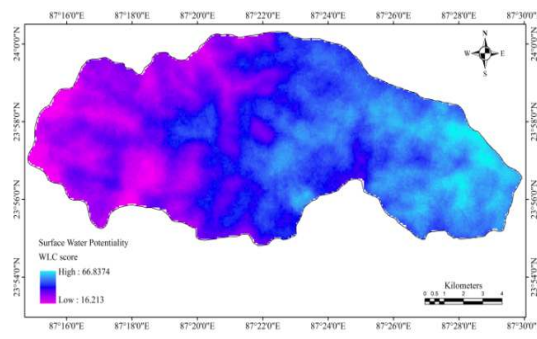


Fig. 4a. Weighted composite surface water potentiality

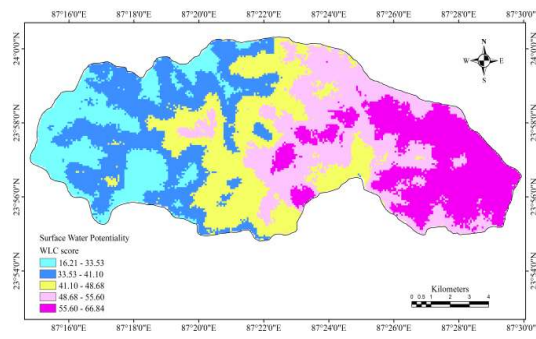


Fig. 4b. Weighted classified surface water potentiality

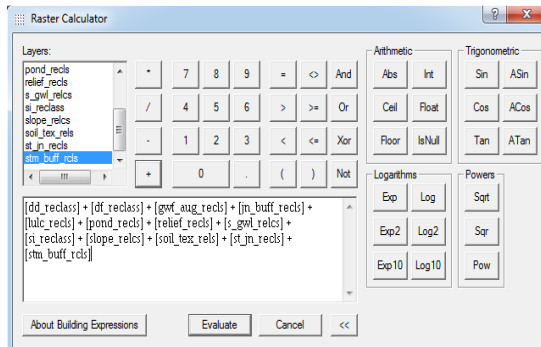


Fig. 5a. Raster calculator with LC of the parameters

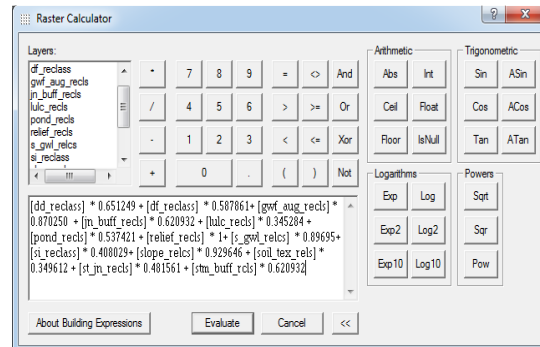


Fig. 5b. Shows the raster calculator with WLC of the parameters

Table 3. Area under different surface water suitability zones (based on un weighted composite score)

Water availability status	Classified score	Number of pixel	Area (sq.km.)	% to total area
Very low	27 - 50	20363	14.16	8.22
Low	50 - 60	17317	37.82	21.95
Moderate	60 - 70	17288	38.05	22.08
High	70 - 80	15963	48.34	28.05
Very high	80 - 98	17817	33.94	19.69

Table 4. Area under different surface water suitability zones (based on weighted composite score)

Suitability status	Weighted composite score	Area extent (sq.km)	% to total area
Very high potentiality	16.21 - 33.53	24.44	14.19
High potentiality	33.53 - 41.12	38.73	22.48
Moderate potentiality	41.12 - 48.69	36.05	20.92
Low potentiality	48.69 - 55.60	38.97	22.61
Very low potentiality	55.60 - 66.84	34.11	19.80

Comparison of results yielded from LC and WLC models it is found that only 13.5% spatial deviation is found. Areal position in LC model of any class is quite scattered than WLC model. Very high potential zone in WLC model is rather clustered than rest one but areal deviation is only 2.1%. So, application of LC model will not be so wrong.

Table 5. Shows the Pearson's correlation coefficient between deriving factors and surface water availability zones

Parameters	Correlation value
Relief	0.90805**
Temporal ground water fluctuation	0.83075**
Seasonal ground water fluctuation	0.85051**
Slope	0.84400**
Drainage density	0.38678**
Drainage frequency	0.27564*
Weighted junction score	0.37889**
Pond	0.31093**

** *r* values are significant at 0.01 level and

* value is significant at 0.05 level

4.1 Driving Factors

Pearson's correlation between WLC model and regulating factors has been calculated for detecting dominant driving factor. It is detected that relief parameter is most dominant regulatory factor ($r=0.908$) followed by ground water fluctuation ($r=0.85$), slope ($r=0.84$) etc. (see Table 5). Drainage parameters are also significantly associated with surface water availability but degree is relatively lower than relief parameters. Stream frequency and density are high in the upper catchment but most of the streams are either 1st or 2nd order and carries water seasonally. Therefore, its degree of association with surface water availability is little bit low. Changes of forest cover and runoff modification is one of the important issues discussed by many a scholars in recent time

[89,90]. From this study, it is found that sick vegetation allows more surface water potentiality runoff (52.826 mm.) than healthier vegetation (43.1914 mm.). It is quite unique but rainfall pattern compels to reflect so. From principal component analysis, it is detected that relief parameter explain 51.4% of the variability of potential surface water availability.

4.2 Estimation of Runoff Volume for Kuskarani Watershed

Figs. 6-8 respectively present the curve number, potential retention capacity and initial abstraction (Ia) which are required for constructing runoff model(s). Curve number of this basin ranges from 70-92 (Fig. 6) and weighted CN of the basin as whole is 67-87. CN is high in the lower part of the basin which is characterized by relatively finer soil, some parts are covered with vegetation, crop land and grass land. Fig. 7 illustrates the spatial maximum retention capacity of the basin where high potential retention is recorded upper part of the basin. Fig. 8 shows that average initial abstraction ranges from 6.6-30.9 mm. with an average of 18.75. Maximum initial abstraction (>24 mm.) is noticed in the upper catchment. Coarser and bare soils are the major vector for such high abstraction. Estimated average annual runoff depth in Kuskarani watershed is 1362.07 mm. and it varies from 1291.09 mm. to 1434.92 mm. over the basin (Fig. 9a) according to the nature of distribution of CN. Fig. 10a shows the continuous runoff depth model and Fig. 9b and Table 6 represents the classified runoff pattern and their respective area. From Table 6 it is clear that 11.27% and 25.58% area of the total basin area is characterized by very high (1393.36mm. to 1434.92 mm.) and high (1372.23 mm.-1393.96 mm.) runoff depth zones respectively and these are mostly located in the lower, lower middle and left wings of the main river. Spatial rainfall association is one of the main reasons behind such runoff pattern. As most of the periods of a year do not receive rain and even the intensity of

rainfall is not also equal, the antecedent soil moisture condition is not always supports to prompt runoff just after rain and runoff response is not also even. Out of total runoff, maximum runoff yields during monsoon time when rainfall is maximum. Actually, it is possible because AMC on that monsoon period favours least abstractions and supports large scale surface runoff. So, in this region, practically runoff does mean the amount of flow during monsoon and it is 1113.73 mm. (11a) which is 75% of the total rainfall. Pre monsoon period also shows 126.24 mm. runoff (12a) theoretically but practically if

other outputs like evapotranspiration are taken into account, runoff will be 0 in this time. Table 7 and 8 respectively depict the spatial pattern of monsoon and pre monsoon runoff depth and their respective areal concentration. Out of total basin area 9.02% area records very high runoff depth (1,146.069 - 1,182.335 mm.) followed by high runoff depth which covers 25.19% to total area with a runoff depth of 1,124.927 - 1,146.069 mm. during monsoon time(see Table 7). Table 8 shows that 13.82% area is characterized by high runoff depth (146.353 - 163.892 mm.) during pre monsoon time.

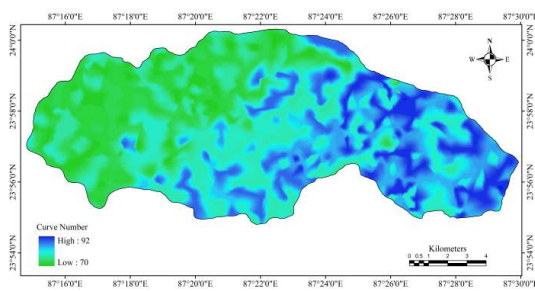


Fig. 6. Spatial pattern of curve number (CN)

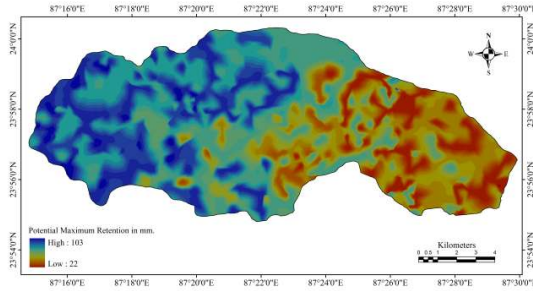


Fig. 7. Spatial pattern of potential maximum retention

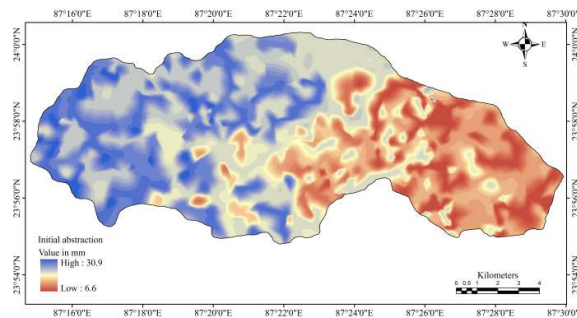


Fig. 8. Initial abstraction pattern

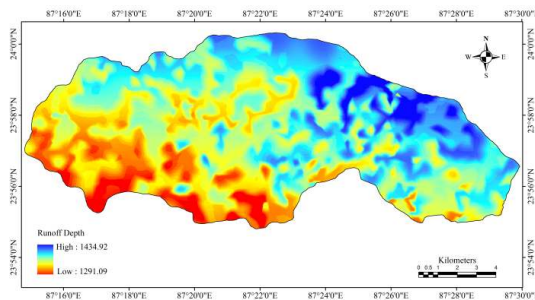


Fig. 9a. Annual average continuous surface runoff depth

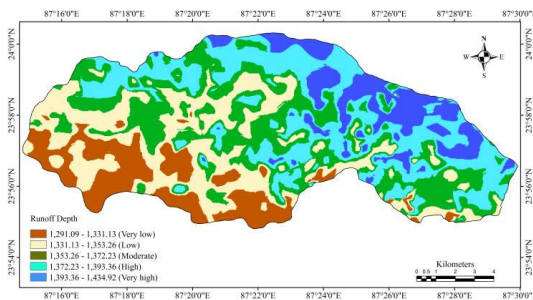
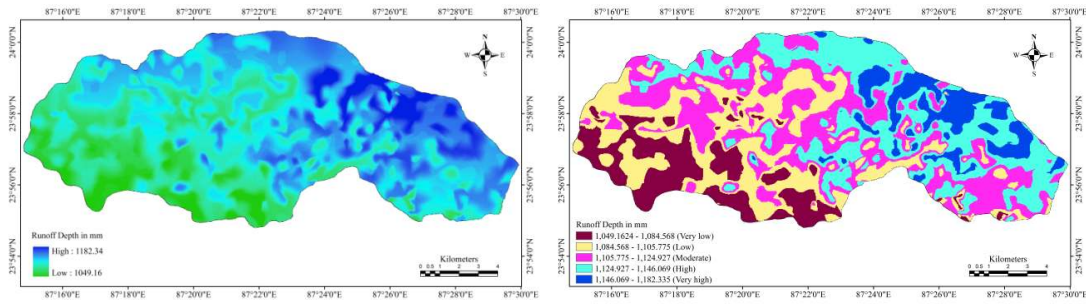


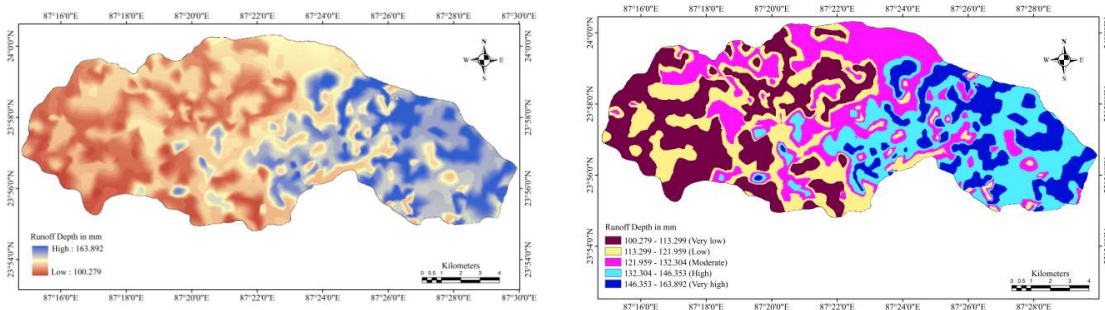
Fig. 9b. Classified average annual surface runoff depth model

Table 6. Spatial annual average runoff depth

Runoff status	Classified score (mm.)	Area extent (sq.km)	% of total area
Very low	1291.09 - 1331.13	23.22	13.48
Low	1331.13 - 1353.26	40.30	23.39
Moderate	1353.26 - 1372.23	45.27	26.27
High	1372.23 - 1393.36	44.09	25.59
Very high	1393.36 - 1434.92	19.43	11.28

**Fig. 10. Spatial runoff depth in monsoon (a) continuous model (b) classified model****Table 7. Area under monsoon runoff depth**

Runoff status	Classified score (mm.)	Area extent (sq.km)	% of total area
Very low	1,049.162 - 1,084.568	23.08	13.40
Low	1,084.568 - 1,105.775	41.44	24.05
Moderate potentiality	1,105.775 - 1,124.927	48.84	28.34
High	1,124.927 - 1,146.069	43.41	25.19
Very high	1,146.069 - 1,182.335	15.54	9.02

**Fig. 11. Spatial runoff depth in pre monsoon (a) continuous model (b) classified model****Table 8. Area under pre monsoon runoff depth**

Runoff status	Classified score (mm.)	Area extent (sq.km)	% of total area
Very low	100.279 - 113.299	40.89	23.73
Low	113.299 - 121.959	35.94	20.86
Moderate	121.959 - 132.304	38.71	22.47
High	132.304 - 146.353	34.66	20.11
Very high	146.353 - 163.892	22.10	12.83

4.3 Impact of Evapotranspiration (ET) on Runoff

Annual potential evapotranspiration (ET) in the study area is about 72cm./year which is almost 50% of the total rainfall. This rate of evaporation strongly varies over seasons, e.g. monsoon pre monsoon months (March to May) yield maximum ET which most of the cases exceeds rainfall. During monsoon time (June to October), this rate of ET is not as strong as during pre monsoon because of >90% relative humidity in air. Still, within monsoon months average ET is 53% of the total rainfall. In pre monsoon time this rate is >80% but this rate largely differs over LULC types. All these information bring another fact in forefront that the amount of runoff depth calculated as per SCS CN is devoid of considering this ET factor and if this factor is incorporated certainly the amount of runoff estimated and plotted in Figs. 12a and 12b; 13a and 13b will be reduced. Estimation and spatial runoff modeling will be more perfect if spatial ET of different periods (Monsoon and pre monsoon) is deducted from the runoff models of respective times. Keeping this unavoidable fact in mind, in this section, ET models of the monsoon and pre monsoon periods have been constructed based on some major vectors of ET like types of LULC, soil types, temperature, wind speed etc. following

FAO 2010 [91]. Growing land use change specifically, change of forest land into agriculture has intensified soil moisture loss and it will negatively affect surface runoff availability.

4.4 Validation of Runoff Model

Calculated RE value and NSE value are respectively 53.65% and 0.6782. RE value established that runoff model is not highly optimum because relative error is 53.65%. Nash-Sutcliffe efficiency (NSE) also indicates the same but the value remains within the range of acceptability (0-1) as stated by Nash and Sutcliffe [87]. Here it is to be mentioned that effective runoff model is valid but the initial model without considering evaporation is not valid in these validation reference scales.

4.4.1 Validation of potential surface water model surface runoff depth model using field based discharge data

Discharge is measured from different stream site and junction sites after constructing potential surface water available zones. Global Positioning System (GPS) based method is used for coordinating map and field site. All total 65 sites have been selected for measuring discharge representing area proportion sampling.

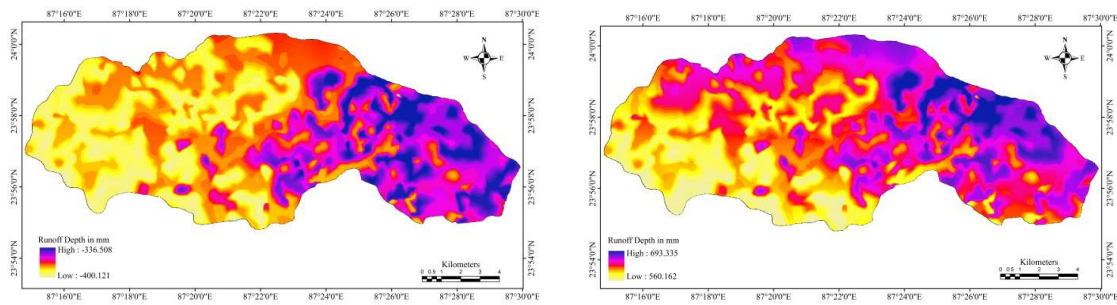


Fig. 12. Effective surface runoff depth (a) pre monsoon (b) monsoon

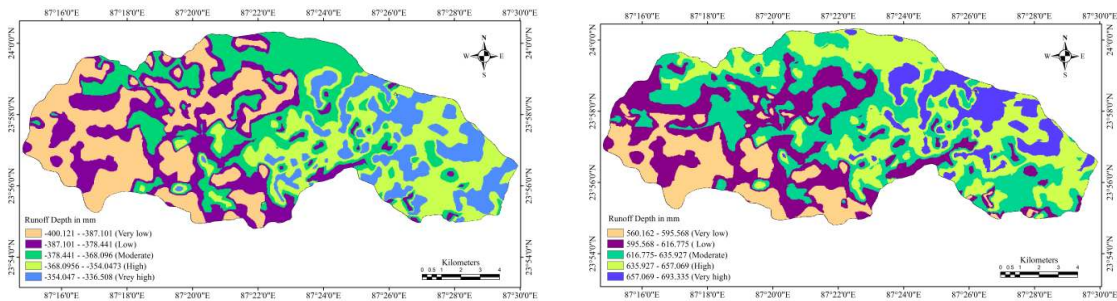


Fig. 13. Classified pattern of effective surface runoff depth (a) pre-monsoon (b) monsoon

4.5 Discharge Conditions

In Table 9, stream strength, discharge availability, level of discharge fluctuation in inter suitability zones and intra suitability zones. In most suitable zone over confluence segment, due to having high strength of streams in term of flow accumulation, both usable water and consistencies of water supply are high. In same suitability class, water availability decreases upstream segments and away from streams. Actual water supply capacity during pre monsoon

period in most suitable zone varies from 61440 to 192650 m³/day if all water is used or 43386 to 130980 m³/day if 30% water is allowed to flow. In monsoon time, water supplying capacity is almost five times greater than premonsoon. It should be noted that estimation is also given for seven days considering the irrigation interval to the crops like pulses, oil seeds mainly cultivated in pre monsoon periods (Table 8). Therefore, estimation of irrigated area using the available water can be done based on cumulative water discharge.

Table 9. Field based measurement of the discharge of streams and accuracy assessment

Suitability status	Nature of river	Discharge (cumec.)	Remarks
Very highly potential zone	3 rd and 4 th order dominated at the confluence 2 nd and 3 rd order dominated at the middle segment	<u>At the confluence:</u> Monsoon: 12.5 cumec Premonsoon: 2.3 cumec. <u>Spatial variation:</u> CV=17.45 to 23.74% <u>At the middle segment:</u> Monsoon: 05.2 cumec Premonsoon: 0.9 cumec. <u>Spatial variation:</u> CV=18.32 to 26.45%	Water can be harvested directly from stream; pre monsoon water harvest should not exceed 61440 to 192650 m ³ /day or 493530 to 1309700 m ³ /7days if all water is used or 43386 to 130980 m ³ /day or 316372 to 866826 m ³ / 7 days if 30% water is allowed to flow.
High potential zone	Either dominated by 2 nd order with few 3 rd order	Monsoon: 4-5.3 cumec Premonsoon: 0.4-1.2 cumec. Spatial variation: CV=17.42 to 29.26% Seepage water supported	Water can be harvested directly from stream or seepage tank can be prepared; premonsoon water harvest should not exceed 51200 to 110960 m ³ /day if all water is used or 231640 to 562602 m ³ /7 days if 30% water is allowed to flow.
Moderately potential zone	Mainly dominated by 1 st and 2 nd order	Monsoon: 1.92-2.2 cumec Premonsoon: 0.24-0.46 cumec. Spatial variation: CV=24.65 to 57.63% Seepage water supported	Water can be harvested directly from stream or seepage tank is necessary to capture water. Water availability: 47% to 68% of the previous class
Low potential	1 st and 2 nd order dominated	Monsoon: 0.16-0.57 cumec Premonsoon: 0-0.07 cumec. Spatial variation: CV=38.76 to 71.54%	Deeper water tank or shallow well can be constructed for water harvesting. High level fluctuation of water supplying potentialities and therefore less certain.
Very low potential zone	1 st order stream dominates	Monsoon: 0 -0.37 cumec Premonsoon: 0 cumec. Spatial variation: CV=18.21 to 34.23%	Surface water potentiality is less, ground water based water harvesting structure can be installed.

Table 10. Regression between Effective runoff depth and actual per day discharge and WLC and discharge

Suitability status (Col 1)	Avg. discharge (cumec./day) (Col 2)	Effective surface runoff (mm.) (Col 3)	WLC (Col 4)	Regression model
Very highly potential zone	12.5	675	38.5	Col 2 vs. Col 3 $y = 8E-14e^{0.048x}$ $R^2 = 0.962$
High potential zone	4.65	646.5	55	Col 2 vs. Col 3 $y = 0.003e^{0.094x}$ $R^2 = 0.953$
Moderately potential zone	2.05	626.6	65	
Low potential	0.3	605.5	75	Col 2 vs. Col 3 $y = 0.314e^{0.008x}$ $R^2 = 0.970$
Very low potential zone	0.15	577.5	89	

So, from this actual availability of water data at different surface water potential zones it is established that high discharge is found at high or very high surface water availability zones. Table 8 clearly depicts the degree and direction of control of surface runoff depth and WLC to actual discharge. High coefficient of determination (0.953-0.962) and regression models as shown in Table 8 represent high degree of positive control. This co linearity of association between field data with constructed model states that the surface water potential model is valid.

Pearson's product moment correlation coefficient value between annual surface runoff and weighted surface water potentiality is 0.52956 which is significant at 0.01 level at one tailed test. Correlation coefficient values are also significant at the same level when it is carried out between monsoon runoff depth and surface water potentiality ($r=0.6453$). So, from these associations it can be inferred that surface water potential model maintains parallelism with surface runoff depth.

Table 10 represents average discharge of different surface water potential zones and their respective effective runoff depth and weighted linear combination score for deriving surface water potentiality. Regression carried out between average discharge and WLC and average discharge and effective runoff depth prove that effective runoff depth strongly control actual discharge of rivers; surface water potential area also yields high discharge in ground reality. Positive regression models and high coefficient of determination in both the cases ($R^2=0.953-0.970$) fortify the above statement. This analysis supports partial application of such runoff model preparation in for finding out suitable surface water harvesting sites and detecting water harvesting sites.

5. CONCLUSION

Surface water potential model shows more expected results than runoff depth model but discharge pattern validates both the models. For increasing the level of acceptability of SCS CN based runoff model more perfectly rainfall should be measured from adequate number of meteorological stations. Necessarily, la value should be refined at per present situation. Besides such limitations of this paper, the suitable sites highlighted by surface water potential model are concomitant with ground reality. Very high and high potential zones recorded maximum river discharge. So, this model can provide decision support for surface water harvesting based planning.

COMPETING INTERESTS

Authors have declared that no competing interests exist.

REFERENCES

1. IPCC. Intergovernmental panel on climate change. Internet html document; 1998. Available: <http://www.ipcc.ch/>
2. IPCC. Intergovernmental panel on climate change. Internet Html Document; 2007. Available: <http://www.ipcc.ch/>
3. Chakraborty A. Study on growth of major crops in Birbhum district. Scholars Journal of Veterinary Science. 2015;2(1B): 63-66.
4. Mooley DA, Partasarathy B, Sontakke NA. Relationship between all India summer monsoon rainfall and southern oscillation/eastern equatorial Pacific sea surface temperature. Proceedings of the Indian Academy of Science- Earth and Planetary Sciences. 1985;94(3):199-210.

5. Sanndipan Ghose, Biswaranjan Mistri. Geographic concerns on flood climate and flood hydrology in monsoon-dominated Damodar River Basin, Eastern India. *Geography Journal*. 2015;(2015):1-16. Article ID 486740. Available:<http://dx.doi.org/10.1155/2015/486740>
6. Ray A, Shekhar S. Ground water issues and development strategies in West Bengal, Bhu-Jal News. Central Ground Board. 2009;24(1):1-2.
7. Das P. Hydro geomorphic characteristics of Kuya River Basin in Eastern India and their impact on agriculture and settlement, Ph. D. thesis submitted in Visva-Bharati, Santiniketan, West Bengal. 2014;181-185.
8. Sen S. The importance of drainage in agriculture of West Bengal, a publication of the Geographical Institute, Presidency College, Calcutta. 1970;80-81.
9. Pal S, Akoma OC. Water scarcity in wetland area within Kandi block of West Bengal: A hydro-ecological assessment. *Ethiopian Journal of Environmental Studies and Management*. 2009;2(3):1-17.
10. Pal S. River Flood: Dynamics Detection and Prediction, LAP, Germany; 2011.
11. Stuebe MM, Johnston DM. Run-off volume estimation using GIS techniques. *J Am Water Resour Assoc*. 1990;26:611–620.
12. Ponce VM, Hawkins RH. Runoff Curve Number: Has it reached maturity? *J Hydrol Eng*. 1996;1:11–19.
13. Mishra SK, Singh VP. SCS-CN based hydrological simulation package, In: mathematical models in small watershed hydrology and applications (eds). Water Resources Publications. CO; 2002;391-464. Littleton.
14. Michel C, Vazken A, and Perrin C. Soil conservation service curve number method: How to mend a wrong soil moisture accounting procedure. *Water Resour Res*. 2005;41:1–6.
15. Schneider LE, McCuen RH. Statistical guidelines for curve number generation. *J Irrig Drain Eng*. 2005;131:282–290.
16. Zhan X, Huang M. Arc CN-runoff: An Arc GIS tool for generating curve number and run-off maps. *Environ Model Softw*. 2004;19:875–879.
17. Tessema SM, Lyon SW, Setegn SG, Mortberg U. Effects of different retention parameter estimation methods on the prediction of surface runoff using the SCS curve number method. *Water Resour Manage*. 2014;28(10):3241–3254.
18. Awadallah AG, Saad H, Elmoustafa A, Hassan A. Reliability assessment of water structures subject to data scarcity using the SCS-CN model. *Hydrol Sci J*; 2015. DOI: 10.1080/02626667.2015.1027709
19. Khare D, Patra D, Mondal A, and Kundu S. Impact of landuse/land cover change on run-off in a catchment of Narmada river in India. *Appl Geomat*. 2015;7(1):23–35.
20. Nayak TR, Jaisawal RK. Rainfall-runoff modelling using satellite data and GIS for Bebas river in Madhya Pradesh. *J Inst Eng*. 2003;84:47–50.
21. Wang Q, Takahashi H. A land surface water deficit model for an arid and semiarid region: impact of desertification on the water deficit status in the Loess Plateau, China, *Journal of Climate*. 1999;12:244-257.
22. Teeuw R. Groundwater exploration using remote sensing and a low cost geographic information system. *Hydrogeology Journal*. 1995;3:21-30.
23. Sander P, Chesley M, Minor T. Groundwater assessment using remote sensing and GIS in a rural groundwater project in Ghana: Lessons learned. *Hydrogeology*. 1996;4:78-93.
24. Das D. GIS application in hydrogeological studies; 2000. Available:<http://www.gisdevelopment.net/application/nrm/water/overview/wato0003.htm> (Accessed March 2010)
25. Joerin F, Theriault M, Musy A. Using GIS and outranking multicriteria analysis for land-use suitability assessment. *Int. J. Geogr. Inform. Sci*. 2001;15(2):153–174.
26. Vijith H. Ground water potential in the hard rock terrain of Western Ghats. A case study from Kottayam district, Kerala using resourcesat (IRS-P6) data and gis techniques. *Journal of Indian society of Remote Sensing*. 2007;35(2):171-179.
27. Kumar D, Dev P. Groundwater potential zone identification of Karwi Area, Mandakini River Basin, Uttar Pradesh using remote sensing and GIS techniques. *International Journal of Engineering Science Invention*. 2014;3(11):10-19.
28. Laudon H, Sjöblom V, Buffam I, Seibert J, Morth M. The role of catchment scale and landscape characteristics for runoff generation of boreal streams. *Journal of Hydrology*. 2007;344(3–4):198–209.

29. Grabs T, et al. Modeling spatial patterns of saturated areas: A comparison of the topographic wetness index and a dynamic distributed model. *Journal of Hydrology*. 2009;373:15–23.
30. Pereira JMC, Duckstein L. A multiple criteria decision-making approach to GIS-based land suitability evaluation. *International Journal of Geographical Information Systems*. 1993;7(5):407–424.
31. Store R, Kangas J. Integrating spatial multi-criteria evaluation and expert knowledge for GIS-based habitat suitability modelling. *Landscape and Urban Planning*. 2001;55(2):79–93.
32. Bonham Carter GF. *Geographic information systems for geoscientists: Modeling with GIS*. Pergamon Press, New York; 1994.
33. Cambell JC, Radke J, Gless JT, Whirtshafter RM. An application of linear programming and geographic information systems: Cropland allocation in antigue. *Environment and Planning A*. 1992;24: 535–549.
34. Kalogirou S. Expert systems and GIS: an application of land suitability evaluation. *Computers. Environment and Urban Systems*. 2002;26(2–3):89–112.
35. Malczewski J. GIS-based land-use suitability analysis: A critical overview. *Progr. Plann*. 2004;62(1):3–65.
36. Miller W, Collins, WMG, Steiner FR, Cook E. An approach for greenway suitability analysis. *Landscape and Urban Planning*. 1998;42(2–4):91–105.
37. Moreno D, Seigel M. A GIS approach for corridor siting and environmental impact analysis. *GIS/LIS'88. Proceedings from the third annual international conference*. San Antonio, Texas. 1988;2:507–514.
38. Eastman JR, Kyem PAK, Toledano J, Jin W. *GIS and Decision Making*. UNITAR, Geneva; 1993.
39. Church RL. *Geographical information systems and location science*. *Computers and Operations Research*. 2002;29(6): 541–562.
40. Janssen R, Rietveld P. Multicriteria analysis and geographical information systems: an application to agricultural land use in the Netherlands. In: Scholten HJ, Stillwell JCH, (Eds.), *geographical information systems for urban and regional planning*. Kluwer Academic Publishers, Dordrecht. 1990;129–139.
41. USDA. *Urban hydrology for small watersheds; technical releases 55*, Natural resources conservation services. Conservation Engineering Divisions; 1986.
42. Rao KV, Bhattacharya AK, Mishra K. Runoff estimation by curve number method- case studies. *Journal of Soil and Water Conservation*. 1996;40:1-7.
43. Ramakrishnan D, Bandyopadhyay A, Kusuma KA. SCS-CN and GIS-based approach for identifying potential water harvesting sites in the Kali Watershed, Mahi River Basin, India. *Journal of Earth System Science*. 2009;118(8):355–368.
44. Bagchi K, Mukerjee KN. Diagnostic survey of West Bengal(s), dept. of geography. Calcutta University, Pantg Delta & Rarh Bengal. 1983;17-19:42-58.
45. Chakrabarty SC. Some consideration on the evolution of physiography of Bengal, in Chattopadhyay B. (ed.), *West Bengal, Geog. Inst., Presidency College, Calcutta*. 1970;20.
46. Jha VC. Laterite and landscape development in tropical lands, a case study. In: Nag, P.; Kumara, V.; Singh, J. (Ed). *Geography and Environment, Concept*. 1996;112-144.
47. Jha VC, Kapat S. Gully erosion and its implications on land use, a case study. In JHA, V.C. (Ed). *Land degradation and desertification*. Publ., Jaipur and New Delhi. 2003;156-178.
48. Jha VC, Kapat S. Rill and gully erosion risk of lateritic terrain in South-Western Birbhum District, West Bengal, India. *Soc. Nat*. 2009;21:2. (Online) Uberlandia.
49. Wentworth CK. A simplified method of determining the average slope of land surfaces. *American Journal of Science*. 1930;21:184-194.
50. Parthasarathy B, Sonkakke NA, Kothawale DR. Probabilities of droughts and floods over India during the southwest monsoon season. *Curr. Sci*. 1984;53:94–96.
51. *English Indices of Multiple Deprivation (IMD); 2015*. Available: www.cambridgeshireinsight.org.uk
52. Carver SJ. Integrating multi-criteria evaluation with geographical information systems. *International Journal of Geographical Information Systems*. 1991; 5(3):321–339.
53. Eastman JR. *Idrisi for windows, version 2.0: Tutorial exercises*, graduate school of

- geography—Clark University, Worcester, MA; 1997.
54. Banai R. Fuzziness in geographic information systems: Contributions from the analytic hierarchy process. *International J. Geogr. Inform. Syst.* 1993; 7(4):315–329.
55. Heywood I, Oliver J, Tomlinson S. Building an exploratory multi-criteria modelling environment for spatial decision support. In: Fisher, P. (Ed.), *Innovations in GIS*, Taylor & Francis, London. 1995;2:127–136.
56. Jankowski P. Integrating geographical information systems and multiple criteria decision making methods. *International J. Geogr. Inform. Syst.* 1995;9(3):251–273.
57. Barredo JI, Benavides A, Hervhl J, van Westen CJ. Comparing heuristic landslide hazard assessment techniques using GIS in the Tirajana basin, Gran Canaria Island, Spain. *International J. Appl. Earth Observ. Geoinform.* 2000;2(1):9–23.
58. Beedasy J, Whyatt D. Diverting the tourists: Aspatial decisionsupport system for tourism planning on a developing island. *J. Appl. Earth Observ. Geoinform.* 1999;3(4):163–174.
59. Malczewski J. GIS-based land-use suitability analysis: A critical overview. *Progr. Plann.* 2004;62(1):3–65.
60. Asproth V, Holmberg SC, Hakansson A. Decision support for spatial planning and management of human settlements. In: *International institute for advanced studies in systems research and cybernetics*. In: Lasker, G.E. (Ed.), *Advances in Support Systems Research*. Windsor, Ont., Canada. 1999;5:30–39.
61. Jiang H, Eastman JR. Application of fuzzy measures in multi-criteria evaluation in GIS. *Int. J. Geogr. Inform. Syst.* 2000;14: 173–184.
62. Makropoulos C, Butler D. Spatial ordered weighted averaging: Incorporating spatially variable attitude towards risk in spatial multi-criteria decision-making. *Environ. Modell. Software.* 2005;21(1):69–84.
63. Malczewski J, Chapman T, Flegel C, Walters D, Shrubsole D, Healy MA. GIS-multicriteria evaluation with ordered weighted averaging (OWA): Case study of developing watershed management strategies. *Environ. Plann.* 2003;35(10): 1769–1784.
64. Malczewski J, Rinner C. Exploring multicriteria decision strategies in GIS with linguistic quantifiers: A case study of residential quality evaluation. *J. Geogr. Syst.* 2005;7(2):249–268.
65. J Ronald Eastman. Idrisi Andes. Guide to GIS and Image Processing. 2006;87-131.
66. Yager RR. On order Jed weighted averaging aggregation operators in multi-criteria decision making. *IEEE Trans. Syst. Man Cybernet.* 1988;18(1):183–190.
67. Mendes JFG, Motizuki WS. Urban quality of life evaluation scenarios: The case of Sao Carlos in Brazil. *CTBUH Rev.* 2001; 1(2):1–10.
68. Rasmussen BM, Melgaard B, Kristensen B. GIS for decision support—designation of potential wetlands. In: *The Third International Conference on Geospatial Information in Agriculture and Forestry*, Denver, USA; 2001.
69. Araujo CC, Macedo. Multicriteria geologic data analysis for mineral favorability mapping: Application to a metal sulphide mineralized area, Ribeira Valley Metallogenic Province Brazil. *Nat. Resour. Res.* 2002;11:29–43.
70. Malczewski J, Chapman T, Flegel C, Walters D, Shrubsole D, Healy MA. GIS-multicriteria evaluation with ordered weighted averaging (OWA): Case study of developing watershed management strategies. *Environ. Plann.* 2003;35(10): 1769–1784.
71. Rashed T, Weeks J. Assessing vulnerability to earthquake hazards through spatial multicriteria analysis of urban areas. *Int. J. Geogr. Inform. Sci.* 2003;17(6):547–576.
72. Calijuri ML, Marques ET, Lorentz JF, Azevedo RF, Carvalho CAB. Multi-criteria analysis for the identification of waste disposal areas. *Geotech. Geol. Eng.* 2004;22(2):299–312.
73. Rinner C, Malczewski J. Web-enabled spatial decision analysis using ordered weighted averaging. *J Geogr. Syst.* 2002; 4(4):385–403.
74. Gilley JE, Finkner SC, Varvel GE. Slope length and surface residue influences on runoff and erosion, biological systems engineering: Papers and Publications. 1987; Paper 121.
Available:<http://digitalcommons.unl.edu/bio sysengfacpub/121>
75. Brakebill JW, Wolock DM, Terziotti SE. Digital hydrologic networks supporting applications related to spatially referenced

- regression modeling. American Water Resources Association. 2011;47:5.
76. Wang D, Hagen SC, Alizad K. climate change impact and uncertainty analysis of extreme rainfall events in the Apalachicola River basin, Florida. J. Hydrol. 2013;480: 125–135
DOI: 10.1016/j.jhydrol.2012.12.015
 77. Vsevolozhsky VA, Zektser IS. Surface and ground water interaction. Hydrological Cycle 1. Source online.
 78. Leeper GW, Uren NC. Soil Science: an Introduction, 5th edn. Melbourne University Press, Melbourne; 1993.
 79. Costa A, et al. Water retention and availability in soils of the state of santa catarina-brazil: Effect of textural classes, soil classes and lithology. R. Bras. Ci. Solo. 2013;37:1535-1548.
 80. Aswathy MV, Vijith H, Satheesh R. Factors Influencing the Sinuosity of Pannagon River, Kottayam, Kerala, India: An assessment using remote sensing and GIS. Article in Environmental Monitoring and Assessment; 2008.
DOI: 10.1007/s10661-007-9755-6
 81. Huntington JL, Niswonger RG. Role of surface-water and groundwater interactions on projected summertime streamflow in snow dominated regions: An integrated modeling approach. Water resource research. 2012;48(11):1-20.
 82. Horton RF. Drainage basin characteristics. Trans Am. Geo. 1932;13(1):350-361.
 83. Jansen BJ, Booth D, Spink. A determining the informational, navigational, and transactional intent of web queries. Information Processing & Management. 2008;44(3):1251–1266.
 84. US department of agriculture Soil Conservation Service. National Engineering Handbook, section 4, Hydrology. US Government Printing Office, Washinton, DC. 1972;544.
 85. Tekeli TI, Akgul S, Dengiz O, Akuzum T. Estimation of flood discharge for small watershed using SCS curve number and geographic information system. Paper presented at the International Congress on River Basin Management; 2007.
Available: <http://www.pechlivanidis-hydro.com/rainfall-runoff-tools/scs-cn/>
 86. Lawrence AJ, Fennessey PE, Richard H, Hawkins PE. The NRCS curve number, a new look at an old tool. Department of Civil and Environmental Engineering 800 Lancaster Avenue, Villanova, Pennsylvania. 2001;19085-1681(610): 519-4960.
 87. Nash JE, Sutcliffe JV. River flow forecasting through conceptual models. Part I. A discussion of principles. J. Hydrol. 1970;10(3):282–290.
 88. Moriasi DN, Arnold JG, Van Liew MW, Bingner RL, Harmel RD, Veith TL. Model evaluation guidelines for systematic quantification of accuracy in watershed simulations. Tran. ASABE. 2007;50(3): 885–900.
 89. Ginxue Wang, Hidenori Takahashi. A land surface water deficit model for an arid and semiarid region: Impact of desertification on the water deficit status in the loess plateau, China. Laboratory of Geoecology, Graduate School of Environmental Earth Science, Hokkaido University, Sapporo, Japan. 1998;12:144-157.
 90. Jarbou AB, Mohamed E, Amal YA, Hanaa KG, Ahmad KH, Ebtisam A. Soil erosion estimation using remote sensing techniques in Wadi Yalamlam Basin, Saudi Arabia. Advances in Materials Science and Engineering. 2016;1-8. Article ID 9585962. Available: <http://dx.doi.org/10.1155/2016/9585962>
 91. FAO. AQUASTAT online database; 2010. Available: <http://www.fao.org/nr/aquastat>

© 2016 Khatun and Pal; This is an Open Access article distributed under the terms of the Creative Commons Attribution License (<http://creativecommons.org/licenses/by/4.0>), which permits unrestricted use, distribution, and reproduction in any medium, provided the original work is properly cited.

Peer-review history:
The peer review history for this paper can be accessed here:
<http://sciencedomain.org/review-history/15430>